Supplementary Material: Multiscale virtual screening optimization for shotgun drug repurposing using the CANDO platform

Matthew L. Hudson[1] and Ram Samudrala[1, *]

[1]Department of Biomedical Informatics, Jacobs School of Medicine and Biomedical Sciences at the University at Buffalo, State University of New York, Buffalo, New York 14203, United States

[*]Corresponding Author: ram@compbio.org, (716) 888-4858

April 15, 2021

Figure 1: **Comparison of drug-indication pair rankings for two CANDO platform pipelines.** For each pipeline, 13,746 drug indication pairs are ranked relative to each other along each axis. Points (which may overlap) denote a drug-indication pair plotted according to its corresponding rank value in each pipeline. The panels depict the total distribution of rankings, as well as different subsets, at linear and log scales. Panel (a) depicts the ranking of all drug-indication pairs, and (b) is the same distribution plotted on a logarithmic scale. (c) depicts two subsets plotted on linear and logarithmic scales of the drug-indication ranking distribution of each pipeline containing highly ranked drug-indication pairs (each drug-indication pair ranked higher than 373 and 100 for each pipeline). (d) depicts subsets of the ranking distribution where each pipeline ranked a drug substantially highly in at least one pipeline but not necessarily the other (i.e. higher than 100 for one pipeline and any rank for the second pipeline). The highest density region of the drug-indication pair rankings distribution indicates pairs that are ranked relatively high by each pipeline. There is substantial consensus between each pipeline in terms of ranking pairs relatively highly. However, the asymmetric distribution of many pairs (particularly those that are ranked at a high accuracy threshold for only one pipeline) suggests some differentiation on a per drug-indication pair basis, giving rise to per indication differences and contributing to the enhanced performance of the hybrid decision pipeline.

(a) **Ranking of all drug-indication pairs for two pipelines.**

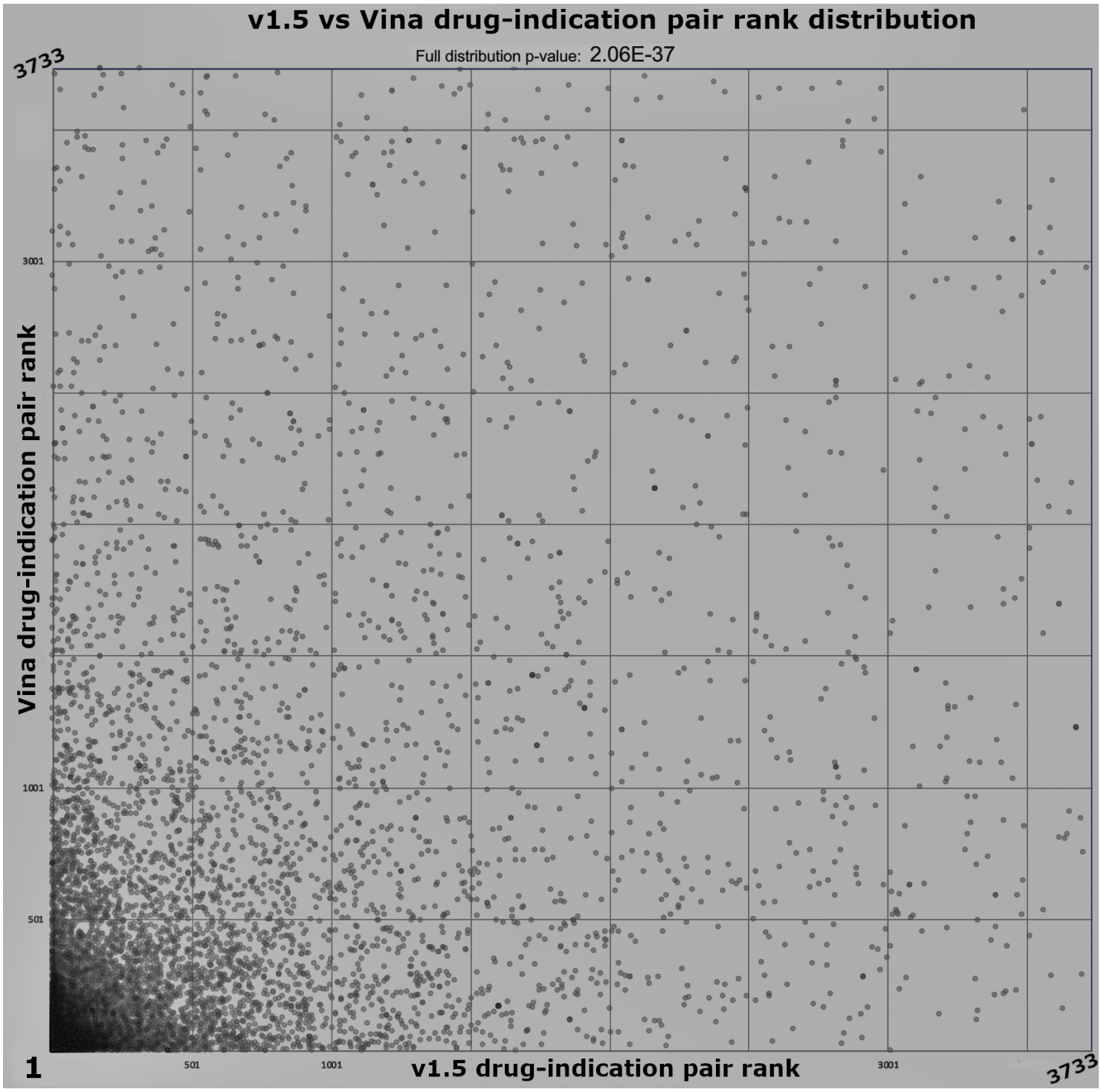

(b) **Drug-indication ranks for two pipelines on a logarithmic scale.**

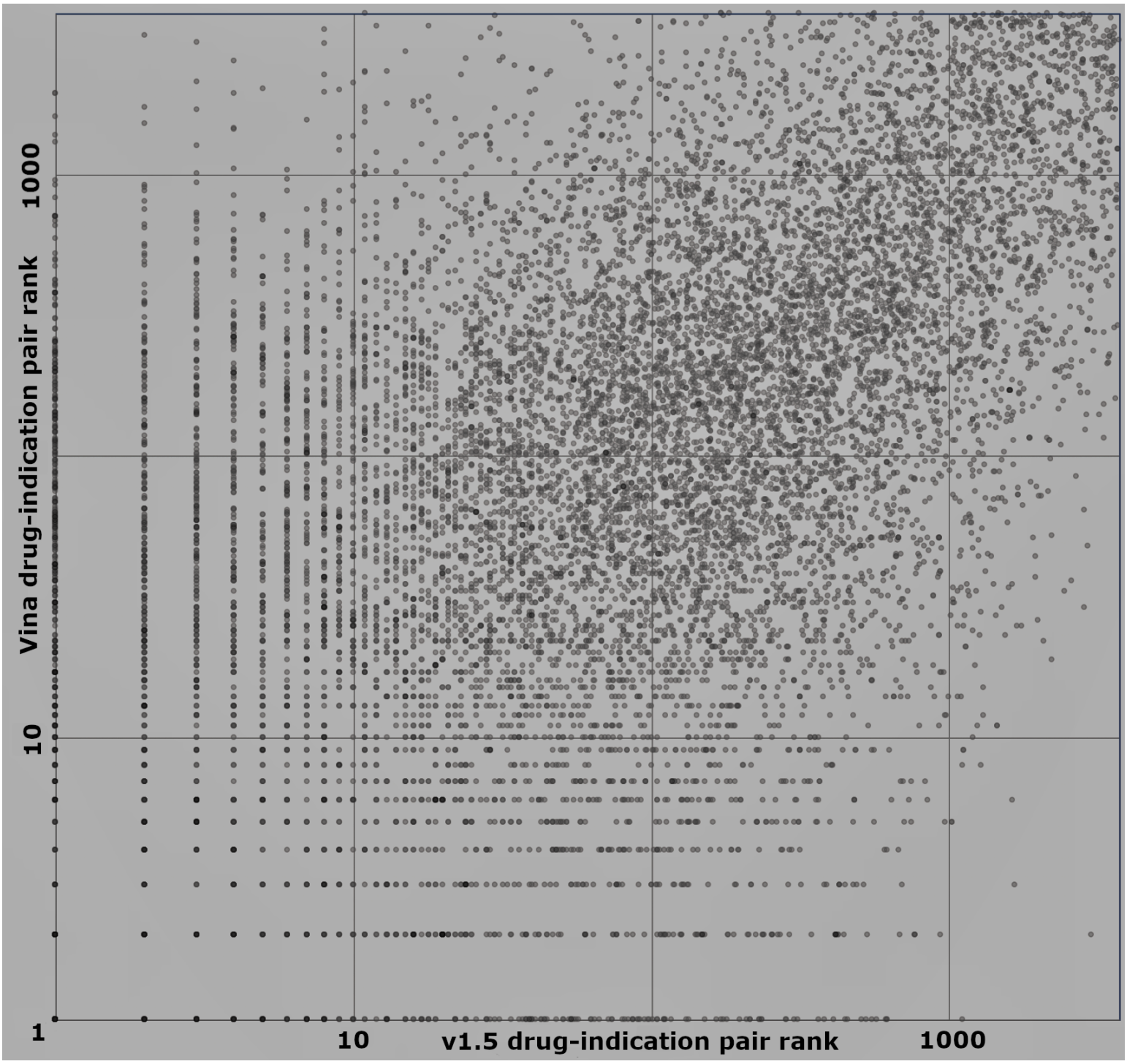

(c) **High ranking drug-indication pair subset distribution.**

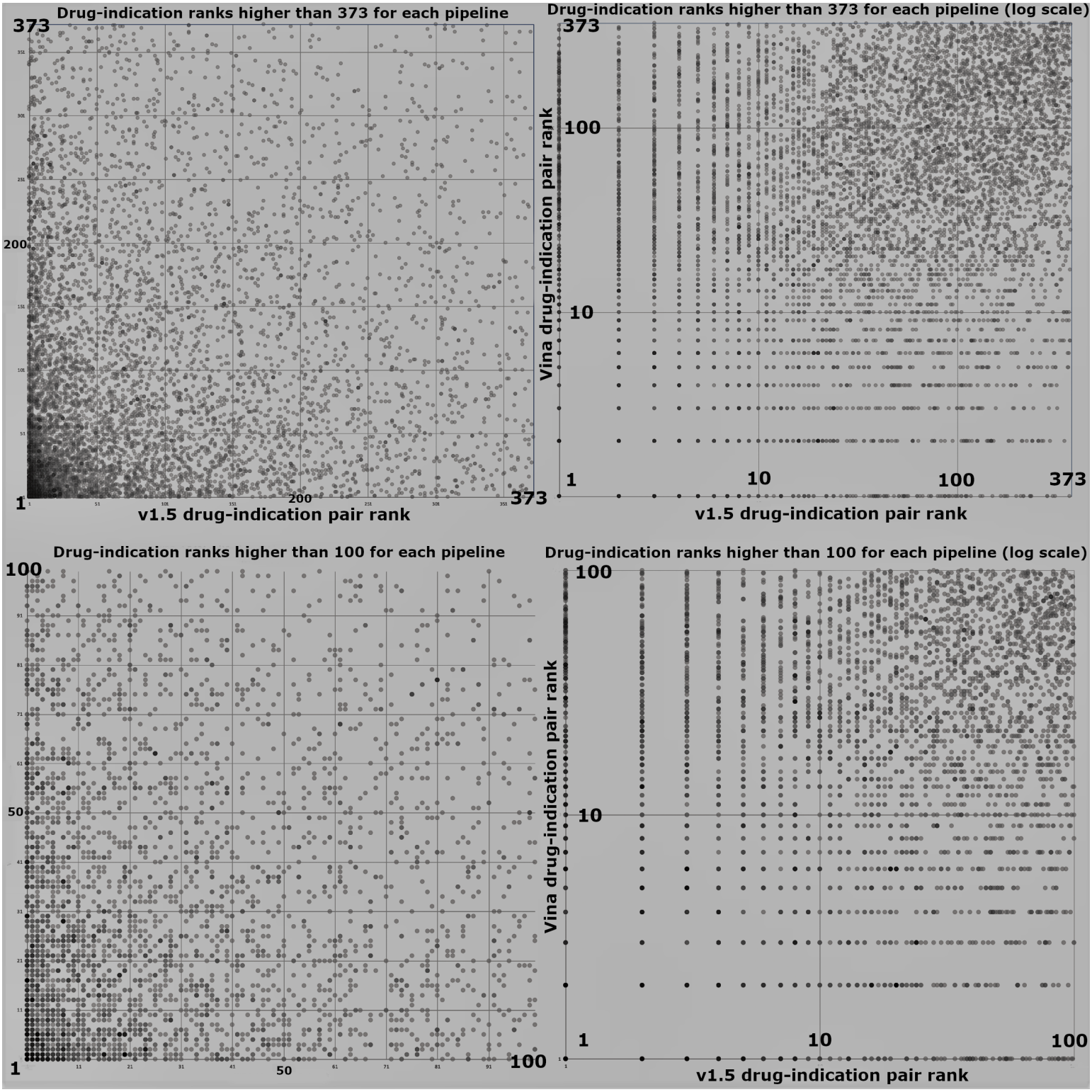

(d) **Subset of drug-indication pairs ranked highly by one pipeline, but not necessarily by the other.**

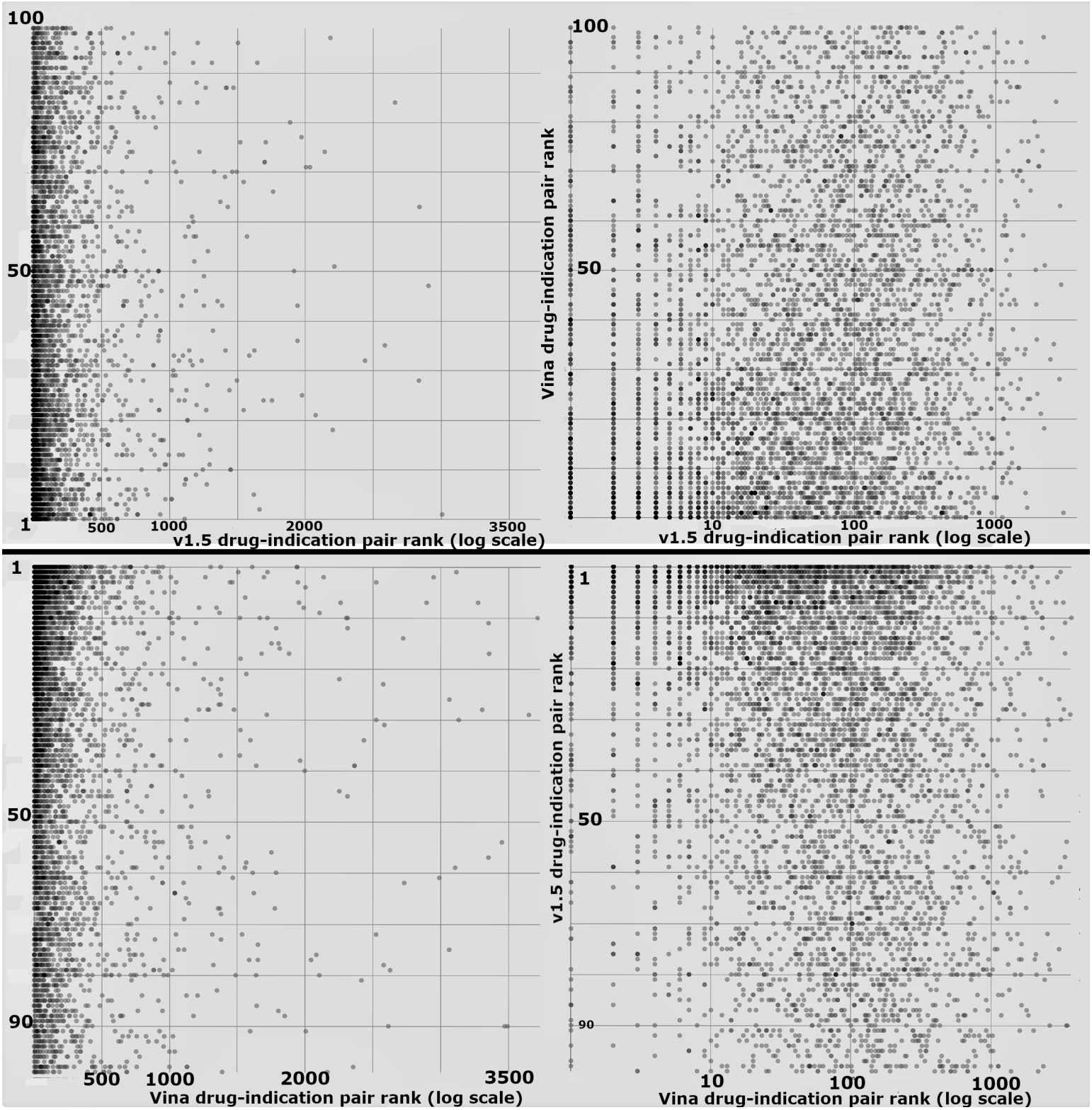

Figure 2: **Indication-indication associations between MeSH Neoplasm associated classes based on the number of compounds predicted in the Top 10 cutoff by the Vina pipeline.** Indication-indication association counts are plotted as a chord diagram for a selection of Top 10 predicted compounds by the Vina pipeline for Neoplasm associated MeSH indication classes. This diagram shows indications related by the number of associated compounds predicted in the Top 10 for each indication. Raw association counts are provided in Supplementary Table 1.

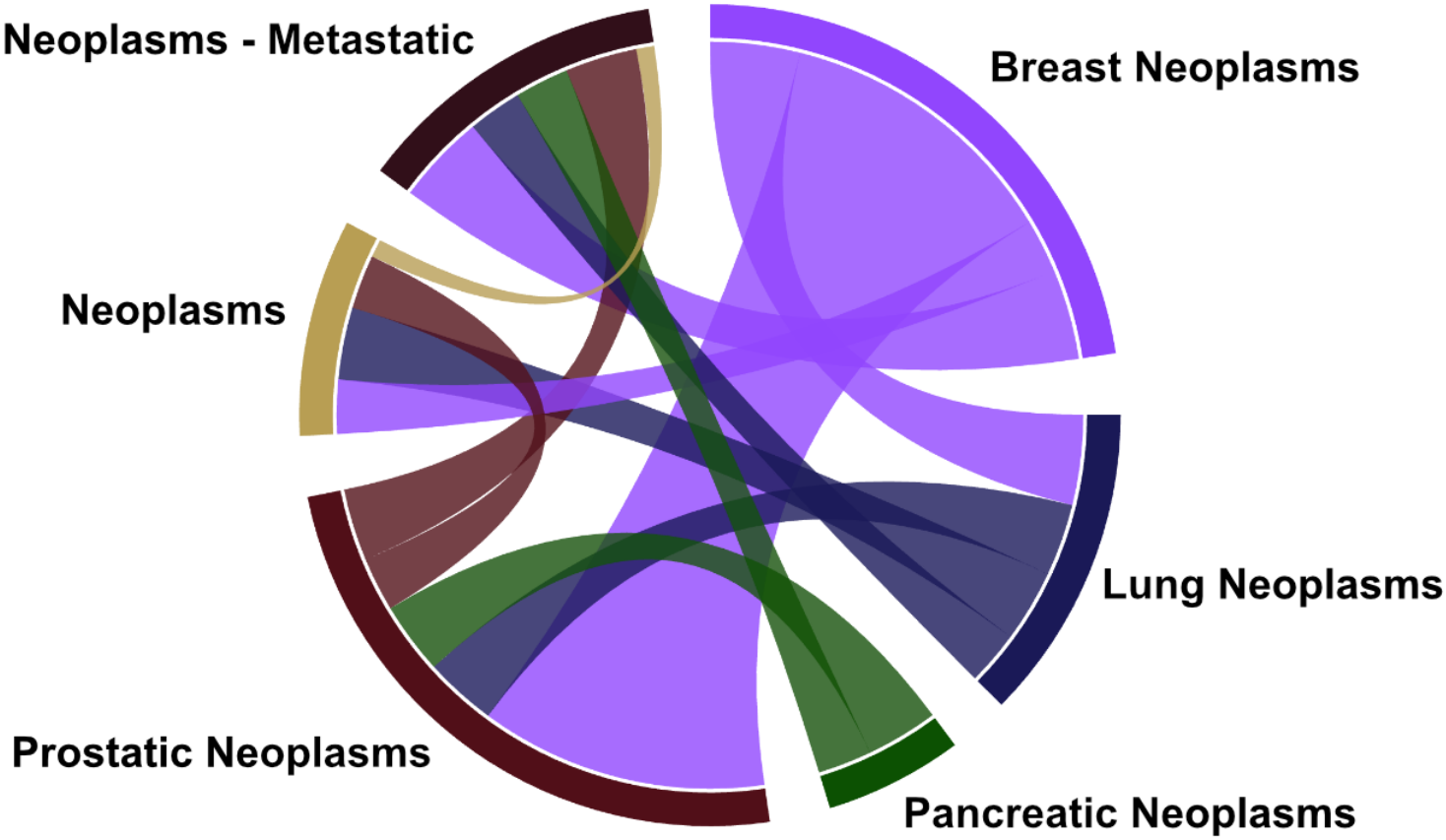

Table 1: **Raw indication-indication association counts** The number of compounds predicted in the Top 10 by the Vina pipeline that each MeSH indication-indication pair share.

MeSH Indication	Breast Neoplasms	Lung Neoplasms	Pancreatic Neoplasms	Prostatic Neoplasms	Neoplasms	Neoplasms - Metastatic
Breast Neoplasms	N/A	5	0	16	3	5
Lung Neoplasms	5	N/A	0	4	4	3
Pancreatic Neoplasms	0	0	N/A	4	0	3
Prostatic Neoplasms	16	4	4	N/A	3	4
Neoplasms	3	4	0	3	N/A	1
Neoplasms - Metastatic	5	3	3	4	1	N/A